



April 2004

# Design of Part Feeding and Assembly Processes with Dynamics

Peng Song

*University of Pennsylvania*, pengs@grasp.cis.upenn.edu

J. C. Trinkle

*Rensselaer Polytechnic Institute*

R. Vijay Kumar

*University of Pennsylvania*, kumar@grasp.upenn.edu

Jong-Shi Pang

*Rensselaer Polytechnic Institute*

Follow this and additional works at: [http://repository.upenn.edu/meam\\_papers](http://repository.upenn.edu/meam_papers)

## Recommended Citation

Song, Peng; Trinkle, J. C.; Kumar, R. Vijay; and Pang, Jong-Shi, "Design of Part Feeding and Assembly Processes with Dynamics" (2004). *Departmental Papers (MEAM)*. 31.

[http://repository.upenn.edu/meam\\_papers/31](http://repository.upenn.edu/meam_papers/31)

Copyright 2004 IEEE. Reprinted from *Proceedings of the 2004 IEEE International Conference on Robotics and Automation (ICRA 2004)*, Volume 1, pages 39-44.

Publisher URL: <http://ieeexplore.ieee.org/xpl/tocresult.jsp?isNumber=29020&page=1>

This material is posted here with permission of the IEEE. Such permission of the IEEE does not in any way imply IEEE endorsement of any of the University of Pennsylvania's products or services. Internal or personal use of this material is permitted. However, permission to reprint/republish this material for advertising or promotional purposes or for creating new collective works for resale or redistribution must be obtained from the IEEE by writing to [pubs-permissions@ieee.org](mailto:pubs-permissions@ieee.org). By choosing to view this document, you agree to all provisions of the copyright laws protecting it.

---

# Design of Part Feeding and Assembly Processes with Dynamics

## **Abstract**

We introduce computational support tools for the analysis and design of systems with multiple frictional contacts, with a focus on applications to part feeding and assembly processes. The tools rely on dynamic models of the processes. We describe two approaches to modeling, the Stewart-Trinkle model [1] and the Song-Pang-Kumar model [2], that allow the designer to experiment with different geometric, material and dynamic properties and optimize the design for performance. In order to accommodate contact transitions, we introduce a smooth cone model for friction. We illustrate the models and the design process by describing the design optimization of a part feeder.

## **Comments**

Copyright 2004 IEEE. Reprinted from *Proceedings of the 2004 IEEE International Conference on Robotics and Automation (ICRA 2004)*, Volume 1, pages 39-44.

Publisher URL:<http://ieeexplore.ieee.org/xpl/tocresult.jsp?isNumber=29020&page=1>

This material is posted here with permission of the IEEE. Such permission of the IEEE does not in any way imply IEEE endorsement of any of the University of Pennsylvania's products or services. Internal or personal use of this material is permitted. However, permission to reprint/republish this material for advertising or promotional purposes or for creating new collective works for resale or redistribution must be obtained from the IEEE by writing to [pubs-permissions@ieee.org](mailto:pubs-permissions@ieee.org). By choosing to view this document, you agree to all provisions of the copyright laws protecting it.

# Design of Part Feeding and Assembly Processes with Dynamics

Peng Song\*, J. C. Trinkle†, Vijay Kumar‡, and Jong-Shi Pang§

\*GRASP Lab, University of Pennsylvania, Philadelphia, PA 19104. Email: pengs@grasp.cis.upenn.edu

†Dept. of Computer Science, Rensselaer Polytechnic Institute, Troy, NY 12180. Email: trink@cs.rpi.edu

‡GRASP Lab, University of Pennsylvania, Philadelphia, PA 19104. Email: kumar@grasp.cis.upenn.edu

§Dept. of Mathematical Sciences, Rensselaer Polytechnic Institute, Troy, NY 12180. Email: pangj@rpi.edu

**Abstract**— We introduce computational support tools for the analysis and design of systems with multiple frictional contacts, with a focus on applications to part feeding and assembly processes. The tools rely on dynamic models of the processes. We describe two approaches to modeling, the Stewart-Trinkle model [1] and the Song-Pang-Kumar model [2], that allow the designer to experiment with different geometric, material and dynamic properties and optimize the design for performance. In order to accommodate contact transitions, we introduce a smooth cone model for friction. We illustrate the models and the design process by describing the design optimization of a part feeder.

## I. INTRODUCTION

There are many manufacturing processes in which nominally rigid bodies undergo frictional contacts, possibly involving impacts. Examples of such processes include part-feeding, assembly, fixturing, material handling, and disassembly. In order to understand the complexity of such processes it is useful to consider the part orienting device shown in Figure 1. A cup-shaped part enters chute “A” in one of two nominal orientations, which we will call “open end up” (on the left) and “open end down” (on the right). The objective of this mechanism is to cause the part to exit chute “C” in the “open end up” configuration regardless of the orientation when entering chute “A”. The part is subject to multiple frictional contacts with the walls of the chutes and the pin “B”. It undergoes frictional impacts before either going down the chute or gets stuck inside the device. There are many factors that affect this feeding process, including the geometry and physical properties of the device and part and the part’s initial condition. Typically, the preliminary design of such systems is based on strong intuition, and the detailed design is refined empirically via prototyping. If the prototype does not function properly, as is usually the case in the first several trials, there is no systematic approach to redesign, because the design constraints of such systems are dominated by unilateral constraints and constant transitions between contact states.

The dynamics of part feeding and assembly processes are notoriously difficult to predict because the dynamic models for systems with unilateral constraints are vastly inadequate, and in some cases, do not exist. This is true even for the case of deterministic models. In the past, geometric and quasi-static approaches have been adopted to planning manipulation [3], [4], [5], [6], assembly [7], [8], part feeding [9], fixturing [10], [11], and grasping tasks [12]. Only now are some of the fundamental underpinnings of systems with multiple frictional

contacts and impacts being explored rigorously [13], [14], [15], [16]. However, there is no systematic approach to planning/design in problems with dynamics [17].

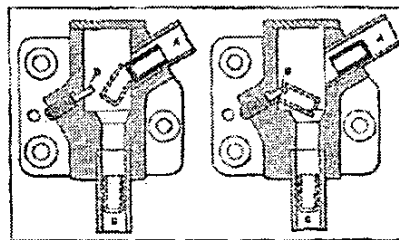
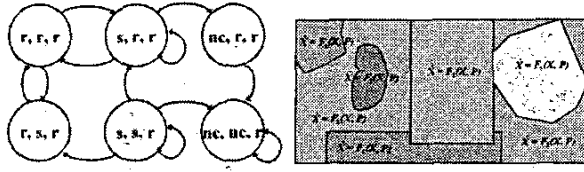


Fig. 1. The exit orientation of the cup-shaped part must be with the open end up, regardless of the entering orientation [18].

In this paper, we introduce a framework for the design of part feeding and automated assembly processes. Our methods rely on the development of dynamic models and optimization of the dynamics with respect to geometric, material and dynamic properties. We describe two dynamic models: the Stewart-Trinkle model [1], which relies on a linear complementary problem (LCP) formulation to handle contact transitions and with an implicit assumption that impacts are inelastic; and an extension of the Song-Pang-Kumar model [2], a more general, nonlinear complementary problem (NCP) model capable of approximating a wide variety of contact conditions including elastic or viscoelastic impacts. Numerical studies on both models are reported in Section IV. In Section V, we illustrate our approach with the design optimization of the part feeding mechanism described in Figure 1.

## II. DESIGN FRAMEWORK

The automatic assembly and part feeding systems can be modeled as switched systems, a special class of hybrid systems in which the state space can be partitioned into  $n_Q \in Q$  non-overlapping regions, each corresponding to a mode of operation characterized by continuous dynamics. The system state in the figure is characterized by a *continuous state*  $X \in \mathbb{R}^n$  and a collection of *discrete modes* or discrete states. Each mode consists of a set of *ordinary differential equations* (ODEs) or *differential algebraic equations* (DAEs) that govern the evolution of the continuous state  $X$  and a set of *invariants* that describe the conditions under which the ODEs or DAEs are valid. The continuous and discrete states are defined as  $(X, Q) \in \mathcal{X} \times \mathcal{Q}$  where  $\mathcal{X} \subset \mathbb{R}^n$  and  $\mathcal{Q}$  is the set of natural



(a) Contact state representation for a system with three contacts (r-rolling; s-sliding; nc-no contact).

(b) The switched dynamical system representation corresponding to the contact states representation above.

Fig. 2. The dynamic equations of motion change as the contact state changes making the resulting time history non smooth.

numbers, with  $Q \in \mathcal{Q}$  denoting the  $Q$ th mode.  $P \in \mathcal{P} \subset \mathbb{R}^k$  is a set of time invariant parameters which appear in the model. These include the geometric parameters, the initial conditions, and the parameters related to the material properties, such as friction, restitution, stiffness, and damping. Exogenous inputs, disturbances and noise are not considered in this paper.

The differential equations in mode  $Q$  are given by:

$$\dot{X} = \mathcal{F}_Q(X, P) \quad (1)$$

Each mode  $Q$  corresponds to a particular assignment of contact conditions (rolling, sliding, or no contact) to each frictional contact. Thus, for a system with  $n_c$  potential contacts, there are  $3^{n_c}$  possible discrete modes, each characterized by a set of conditions in state space. Figure 2 shows the schematic of a switched system with 6 modes.  $\mathcal{F}$  represents the dynamic model that governs the continuous states  $X$  within each mode. The dynamic model may be difficult to obtain in practice. Further, depending on the dynamic model,  $\mathcal{F}$  may not have a unique solution<sup>1</sup>. Under such a circumstance, the representation of states partitions shown in Figure 2 may not be valid or may lead to multivalued solutions. In the next section, we will describe two discrete-time dynamic models. The method we use to develop these models is influenced by the extensive recent work on complementarity problems and time-stepping models for dynamic simulation of rigid-body systems [15], [19], [20].

### III. DYNAMIC MODELS

The dynamic equation of motion for a multibody system with contact interactions can be written in the form

$$M(q)\dot{\nu} = u(t, q, \nu) + W_n(q)\lambda_n + W_t(q)\lambda_t + W_o(q)\lambda_o, \quad (2)$$

where  $q$  is the  $n_q$ -dimensional vector of generalized coordinates,  $\nu$  is the  $n_\nu$ -dimensional vector of the system velocities,  $M(q)$  is the  $n_\nu \times n_\nu$  symmetric positive definite inertia matrix, and  $u(t, q, \nu)$  is the  $n_\nu$ -dimensional external force vector (excluding contact forces).  $\lambda_{n,t,o}$  are the  $n_c$ -dimensional concatenations of the contact forces in the normal direction (labelled  $n$ ) and the two tangential directions (labelled  $t$  and  $o$ ), where  $n_c$  is the number of contacts.  $W_{n,t,o}(q)$  are the  $n_\nu \times n_c$  Jacobian matrices corresponding to the contact forces. The kinematic equations relate the system velocity  $\nu$  to the time-derivative of the system configuration  $\dot{q} \equiv dq/dt$  via a  $n_q \times n_\nu$  parametrization matrix  $G(q)$ :

<sup>1</sup>For a discussion of the uniqueness and existence of solutions for the two models used here, the reader is referred to [1], [2].

$$\dot{q} = G(q)\nu. \quad (3)$$

To complete the formulation of the model, we need to include the contact conditions. In the normal direction, the contact condition of the system is governed by

$$0 \leq \lambda_{in} \perp \phi_{in} \geq 0, \quad i = 1 \dots n_c, \quad (4)$$

where  $\perp$  denotes perpendicularity and  $\phi_{in}$  is the normal separation between contacting objects at the  $i$ th contact.

In the tangential direction, the contact conditions are formulated by requiring that friction forces maximize the energy dissipation rate over the sets of admissible contact forces computed based on the friction model. For Coulomb's quadratic cone, the maximum dissipation principle at the  $i$ th ( $i = 1 \dots n_c$ ) contact can be written as

$$(\lambda_{it}, \lambda_{io}) = \operatorname{argmin} \{ (s_{it}\lambda_{it} + s_{io}\lambda_{io} : (\lambda_{it}, \lambda_{io}) \in \mathcal{FC}(\mu_i\lambda_{in}) \}$$

$$\text{where } \mathcal{FC}(\mu_i\lambda_{in}) \equiv \left\{ (\lambda_{it}, \lambda_{io}) : \sqrt{\lambda_{it}^2 + \lambda_{io}^2} \leq \mu_i\lambda_{in} \right\}, \quad (5)$$

and  $s_i$  represent the slip velocities at the  $i$ th contact. The Coulomb's cone is not differentiable at the origin where  $\mu\lambda_{in} = 0$ . We introduce the following smooth cone to resolve this problem:

$$\mathcal{FC}_\gamma(\mu_i\lambda_{in}) \equiv \left\{ (\lambda_{it}, \lambda_{io}) : \sqrt{\lambda_{it}^2 + \lambda_{io}^2 + \gamma^2} \leq \mu_i\lambda_{in} + \gamma \right\} \quad (6)$$

where  $\gamma \geq 0$  is a small scalar. When  $\gamma = 0$ , the smooth cone (6) converges to the Coulomb's quadratic cone (5) with the assumption that  $0/0 \equiv 0$ . Note that the smooth cone preserves all the properties of the Coulomb's quadratic cone.

However, even for the smooth cone, there is no suitable constraint qualification for the Karush-Kuhn-Tucker (KKT) necessary conditions [21] for the optimization problem when the contact is inactive ( $\lambda_{in} = 0$ ) or when the contact is frictionless ( $\mu_i = 0$ ). To obtain the optimality conditions, we resort to the Fritz John conditions [21].

$$\begin{aligned} 0 \leq \beta_{io} \perp \mu_i\lambda_{in} + \gamma - \sqrt{\lambda_{it}^2 + \lambda_{io}^2 + \gamma^2} &\geq 0 \\ \beta_{io}s_{it} + \frac{\beta_{io}\lambda_{it}}{\sqrt{\lambda_{it}^2 + \lambda_{io}^2 + \gamma^2}} &= 0 \\ \beta_{io}s_{io} + \frac{\beta_{io}\lambda_{io}}{\sqrt{\lambda_{it}^2 + \lambda_{io}^2 + \gamma^2}} &= 0 \\ \beta_{io} &\geq 0, \quad (\beta_{io} \beta_i) \neq 0 \end{aligned} \quad (7)$$

If  $\beta_{io} \neq 0$ , the KKT conditions hold (with the Lagrange multipliers being defined as  $\hat{\beta}_i \equiv \beta_i/\beta_{io}$ ). In a contact problem, we can use  $\mu_i\lambda_{in}$  as a natural choice for  $\beta_{io}$  instead of solving for the extra multiplier. When  $\mu_i\lambda_{in} = 0$ , the Fritz John conditions can be trivially satisfied with a nonzero  $\beta_i$ . These conditions will be used in the next subsection to extend the traditional complementarity conditions to include both active and inactive contact constraints.

The Coulomb's quadratic cone can be linearized using the following polyhedra approximation, at any  $i = 1 \dots n_c$ :

$$\widehat{\mathcal{FC}}(\mu_i\lambda_{in}) \equiv \{ D_i\lambda_{it} : \|\lambda_{it}\|_1 \leq \mu_i\lambda_{in}, \lambda_{it} \geq 0 \} \quad (8)$$

where  $D_i$  is a  $2 \times n_t$  matrix whose columns are coplanar vectors  $d_{i,j}$  ( $j = 1, \dots, n_t$ ) on the plane tangent to the contact

normal (the  $t$ - $o$  plane) and  $n_i$  is the number of edges of the polyhedra. The  $j$ th component of  $\lambda_{if}$  represents the magnitude of tangential force along the  $d_{i,j}$  direction. The polyhedra approximation leads to a linearly constrained problem, thus automatically satisfies the Abadie constraint qualification for the KKT conditions [21]. The following complementarity conditions can be derived from the the maximum dissipation principle problem as:

$$\begin{aligned} 0 &\leq \beta_i e_i + D_i^T s_i \perp \lambda_{if} \geq 0 \\ 0 &\leq \mu_i \lambda_{in} - e_i^T \lambda_{if} \perp \beta_i \geq 0 \end{aligned} \quad (9)$$

where  $e_i$  is a  $n_i$ -vector of ones.

Together, (2), (3), (4), and (7) or (9) constitute the equations of motion which have four components: the dynamics of the mechanical system, the kinematic map, the normal contact conditions, and the friction law.

We consider a time discretization of the differential equations (2) and (3) for  $t \in (0, T]$ . Fix a positive integer  $N$  and let  $h \equiv T/N$ . Partition the interval  $[0, T]$  into  $N$  subintervals  $[t_\ell, t_{\ell+1}]$ , where  $t_\ell \equiv \ell h$ , for  $\ell = 0, 1, \dots, N$ . Write

$$q^\ell \equiv q(t_\ell), \quad \nu^\ell \equiv \nu(t_\ell), \quad \text{and} \quad \lambda_{n,t,o}^\ell \equiv \lambda_{n,t,o}(t_\ell).$$

The time derivatives  $\dot{\nu}$  and  $\dot{q}$  are replaced by the backward Euler approximations: for all  $\ell = 0, \dots, N-1$ ,

$$\dot{\nu}(t_{\ell+1}) \approx \frac{\nu^{\ell+1} - \nu^\ell}{h} \quad \text{and} \quad \dot{q}(t_{\ell+1}) \approx \frac{q^{\ell+1} - q^\ell}{h}.$$

The various time-stepping schemes differ in how  $M(q)$  and the right-hand sides in (2) and (3) are approximated.

In the *fully implicit scheme*, all functions are evaluated at time  $\ell + 1$ . Because the variables such as the inertia matrix and the Jacobians are functions of  $q^{\ell+1}$ , solving for the unknowns  $(q^{\ell+1}, \lambda^{\ell+1})$  involves the solution of nonlinear equations. In contrast, a *semi-implicit scheme* may lead to a linear formulation in terms of  $q^{\ell+1}$ ,  $\nu^{\ell+1}$ , and  $\lambda^{\ell+1}$  at the  $\ell$ th time step.

#### A. A semi-implicit method for rigid contacts with inelastic collisions

Stewart and Trinkle [1] developed a semi-implicit time-stepping model that was originally formulated as a mixed LCP in terms of the unknown state  $(\nu^{\ell+1}, q^{\ell+1})$ , normal and frictional impulses  $(p_n^{\ell+1}, p_f^{\ell+1})$  (defined as:  $p_n^{\ell+1} = h\lambda_n^{\ell+1}$ ,  $p_f^{\ell+1} = h\lambda_f^{\ell+1}$ ), and slack variable  $\beta^{\ell+1}$  approximating the magnitude of the sliding velocity at the contact. However, the state variables can be eliminated by using the equations of motion, thus allowing reformulation of the time-stepping method as a standard LCP( $B, b$ ) written as follows:

$$\begin{aligned} w^{\ell+1} &= B^\ell z^{\ell+1} + b^\ell \\ 0 \leq w^{\ell+1} &\perp z^{\ell+1} \geq 0 \end{aligned} \quad (10)$$

with  $B^\ell$ ,  $b^\ell$ , and  $z^{\ell+1}$  given as follows:

$$\begin{aligned} B^\ell &= \begin{pmatrix} W_n^T M^{-1} W_n & W_n^T M^{-1} W_f & 0 \\ W_f^T M^{-1} W_n & W_f^T M^{-1} W_f & E \\ U & -E^T & 0 \end{pmatrix} \\ b^\ell &= \begin{pmatrix} W_n^T (\nu + M^{-1} u h) + \phi_n(q^\ell)/h \\ W_f^T (\nu + M^{-1} u h) \\ 0 \end{pmatrix}, \quad z^{\ell+1} = \begin{pmatrix} p_n^{\ell+1} \\ p_f^{\ell+1} \\ \beta^{\ell+1} \end{pmatrix}, \end{aligned}$$

where  $E$  is a block diagonal matrix, with each diagonal block equal to a column vector length  $n_i$  with all elements equal to one.  $U$  has the same structure as  $E$  with all elements of the diagonal block equal to  $\mu_i$ , the coefficient of friction at contact point  $i$ . Note that this LCP is only linear because all quantities in  $B$  and  $b$  are computed at time  $t^\ell$ .

Several points are worth noting. First, the term  $\phi_n(q^\ell)/h$  provides constraint stabilization with  $\phi_n(q^\ell)$  being the vector of the normal separations between each pair of bodies in or about to be in contact. When it is negative (implying interpenetration of bodies), it acts to generate a bias impulse that increases the normal component of the relative velocity at a contact be large enough to eliminate the penetration at the end of the next time step. Second, there is no restitution law built into this formulation. To include realistic bouncing effects, one must stop the ST method at the time of each collision and apply an impact model such as Newton's, Poisson's, or Stronge's hypothesis. Third, the usual quadratic friction cone and the noninterpenetration constraints have been linearized in order to obtain a LCP. Fourth, the quantities (such as  $M$  and  $W_n$ ) not superscripted with a time index are assumed to be functions of the known state,  $(\nu^\ell, q^\ell)$ . This is done to ensure the complementarity problem is linear, thus enabling LCP solution techniques. Otherwise, as stated above, the LCP would become a NCP.

#### B. A fully-implicit method with visco-elastic contacts

Song, Pang, and Kumar [2] developed a discrete-time compliant contact model for rigid body simulation. The key idea of this model is to allow local compliance at the contact patch between nominally rigid bodies. Unlike some penalty methods, the compliant model relies on both normal and tangential compliances to model contact forces and can resolve the inconsistencies with uniqueness and existence. In this subsection, we extend the model by using a fully implicit time-stepping scheme. The new model leads to a unified framework for simulation of systems with sustained contacts as well as impacts. We use a lumped viscoelastic model, which is a special case of the distributed compliant model described in [2], to formulate the the contact dynamics. For simplicity, we consider the simplest such model, the Kelvin-Voigt model. At each *potential* contact point  $i$  ( $i = 1, \dots, n_c$ ), we have the following decoupled relations between the contact force  $\lambda$  and the local deformation  $\delta$ , in the  $n$ ,  $t$ , and  $o$  directions respectively:

$$\lambda_{i,n,t,o} = K_{i,n,t,o} \delta_{i,n,t,o} + C_{i,n,t,o} \dot{\delta}_{i,n,t,o}. \quad (11)$$

In the compliant model, the normal separation  $\phi_{in}$  and the tangential slip velocities  $s_{it,o}$  are affected by both the rigid body gross motion and the local deformations:

$$\phi_{in}(q) \equiv \delta_{in} + \Psi_{in}(q), \quad (12)$$

$$s_{it,o} \equiv \dot{\delta}_{it,o} + W_{it,o}^T(q)\nu, \quad (13)$$

where  $\Psi_{in}$  denotes separation caused by the rigid gross motion and  $W_{it,o}$  represents the  $i$ th column of  $W_t$  or  $W_o$ . Note that for rigid body models,  $\phi_{in} \equiv \Psi_{in}$  since  $\delta_{in} \equiv 0$  at a perfectly rigid contact. Writing

$$\delta_{i,n,t,o}^\ell \equiv \delta_{i,n,t,o}(t_\ell), \quad \ell = 0, 1, \dots, N,$$

together with the fully implicit discretization of system dynamics equations (2,3) and the contact constraints (4, 7, 11-13) for all  $i = 1 \dots n_c$ , we have the following discrete-time, mixed nonlinear complementarity problem formulation for dynamics of systems with unilateral constraints:

$$\begin{aligned} \nu^{\ell+1} &= \nu^\ell + hM(q^{\ell+1})^{-1}u^{\ell+1} + hM(q^{\ell+1})^{-1} \\ &\quad [W_n(q^{\ell+1})\lambda_n^{\ell+1} + W_t(q^{\ell+1})\lambda_t^{\ell+1} + W_o(q^{\ell+1})\lambda_o^{\ell+1}] \\ q^{\ell+1} &= q^\ell + hG(q^{\ell+1})\nu^{\ell+1} \\ 0 &\leq \lambda_{in}^{\ell+1} \perp \phi_{in}(q^{\ell+1}) \geq 0 \\ \phi_{in}(q^{\ell+1}) &= \delta_{in}^{\ell+1} + \Psi_{in}(q^{\ell+1}) \\ 0 &\leq \beta_i^{\ell+1} \perp \mu\lambda_{in}^{\ell+1} + \gamma - \sqrt{(\lambda_{it}^{\ell+1})^2 + (\lambda_{io}^{\ell+1})^2} + \gamma^2 \geq 0 \\ \mu\lambda_{in}^{\ell+1} s_{it,o}^{\ell+1} &= -\frac{\beta_i^{\ell+1} \lambda_{it,o}^{\ell+1}}{\sqrt{(\lambda_{it}^{\ell+1})^2 + (\lambda_{io}^{\ell+1})^2} + \gamma^2} \\ s_{it,o}^{\ell+1} &= \frac{\delta_{it,o}^{\ell+1} - \delta_{it,o}^\ell}{h} + W_{it,o}^T(q^{\ell+1})\nu^{\ell+1} \\ \lambda_{i,n,t,o}^{\ell+1} &= \left( K_{i,n,t,o} + \frac{1}{h} C_{i,n,t,o} \right) \delta_{i,n,t,o}^{\ell+1} - \frac{1}{h} C_{i,n,t,o} \delta_{i,n,t,o}^\ell \end{aligned} \quad (14)$$

To illustrate the method, we apply the NCP model (14) to the simulation of a rough spherical body bouncing and rolling on the ground. Depending on the material properties, the ball can undergo one or more frictional impacts and end up in a condition in which it maintains contact with the ground. The model (14) is a unified approach that incorporates all these conditions. The generalized coordinates and the system velocities are given by:

$$\begin{aligned} q &= (x \ y \ z \ e_0 \ e_x \ e_y \ e_z)^T \\ \nu &= (\nu_x \ \nu_y \ \nu_z \ \omega_x \ \omega_y \ \omega_z)^T \end{aligned}$$

where  $(x, y, z)$  are the Cartesian coordinates of the center of mass,  $(e_0, e_x, e_y, e_z)$  are the Euler parameters,  $(\nu_x, \nu_y, \nu_z)$  are the linear velocities along the Cartesian axes, and  $(\omega_x, \omega_y, \omega_z)$  are the angular velocities.

The initial conditions of the object are given by:

$$\begin{aligned} q^0 &= (0 \ 0 \ 0.2 \ 1 \ 0 \ 0 \ 0)^T \\ \nu^0 &= (0.5 \ 0 \ 0 \ 20 \ 0 \ 0)^T \end{aligned}$$

The effective coefficient of restitution for impact for this example is approximately 0.8. An empirical expression of the coefficient of restitution for impacts with the compliant contact

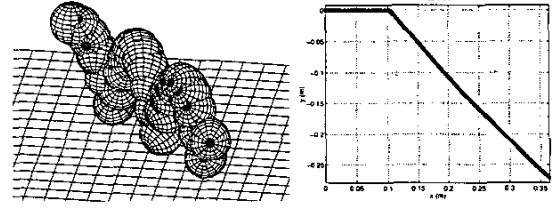


Fig. 3. The trajectory of a rough spherical body with frictional impacts. The object is launched with an initial velocity of 0.5m/s in the x-direction at a height of 0.2m above the horizontal plane and a spin velocity of 20rad/sec around the x-axis. The mass of the ball is  $m = 0.2$ kg and the radius is  $r = 0.05$ m. Other parameters in model (14) include  $h = 2 \times 10^{-4}$ sec,  $N = 5000$ ,  $\gamma = 10^{-8}$ ,  $K = 5 \times 10^4$ N/m, and  $C = 2\sqrt{K}$ sec·N/m.

model can be found in [22]. The NCP is solved by using the AMPL/PATH solver [23] on the NEOS server for optimization at the Argonne National Laboratory. The snapshots of the simulation results and the top view of the motion history at the center of mass are plotted in Figure 3. Applications of this method to more complicated examples including boundary value problems are included in [24].

#### IV. FRICTIONAL IMPACTS

In this section we use the simple example of a rectangular, planar object impacting a horizontal plane to illustrate the modeling of frictional impacts. In this example, there are four potential contacts between the block and the horizontal plane. The maximum number of contact state transitions are  $3^4$ , most of which are geometrically infeasible.

The generalized coordinates of the peg are given by:

$$q = (x \ y \ \theta)^T \quad \text{and} \quad \nu = (\dot{x} \ \dot{y} \ \dot{\theta})^T,$$

where  $(x, y)$  are the coordinates of the center of mass, and  $\theta$  is the orientation of the peg. Other than the contact forces, gravity is the only external force acting on the peg.

$$M(q) = \begin{pmatrix} m & 0 & 0 \\ 0 & m & 0 \\ 0 & 0 & J \end{pmatrix}, \quad G(q) = I_{3 \times 3}$$

$$W_{in}(q) = \begin{pmatrix} 0 \\ 1 \\ x_{vi}(q) - q(1) \end{pmatrix}, \quad W_{it}(q) = \begin{pmatrix} 1 \\ 0 \\ q(2) - y_{vi} \end{pmatrix}$$

where  $(x_{vi}, y_{vi})$  are the coordinates of the  $i$ th vertex,  $i = 1 \dots 4$ . The initial conditions of the peg are set as:

$$q_0 = (0 \ 0.2 \ \pi/4)^T \quad \text{and} \quad \nu_0 = (0 \ 0 \ 0)^T.$$

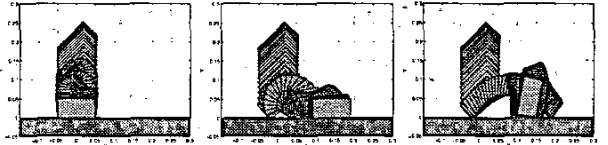


Fig. 4. Simulation of impacts between a rectangular peg and the horizontal plane with three different friction coefficients:  $\mu = 0$  (left),  $\mu = 0.2$  (middle), and  $\mu = 1.0$  (right). The peg is released from still at a distance of 0.2m between the center of mass and the horizontal plane. The mass of the peg is  $m = 0.2$ kg and the inertia  $J = 2 \times 10^{-4}$ kg · m<sup>2</sup>. Other parameters used in this example are given as  $h = 2 \times 10^{-4}$ sec,  $N = 5000$ ,  $\gamma = 10^{-8}$ ,  $K = 5 \times 10^4$ N/m, and  $C = 2\sqrt{K}$ sec·N/m.

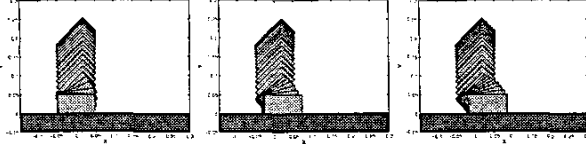


Fig. 5. Inelastic impacts can be predicted by model (14) if we increase the damping ratio to  $C = 200 * \sqrt{K \text{sec-N/m}}$  for the same three cases shown in Figure 4

Figures 4 and 5 show results obtained using the NCP in (14) illustrating both elastic and inelastic impacts as we change the damping ratio associated with the local contact compliance. The results in Figure 5 for inelastic impacts closely match the results obtained from the LCP in (10) (not included in this paper).

### V. DESIGN OF THE PART FEEDING MECHANISM

Figure 6 shows a reorienting mechanism with 12 design variables. The variables are as follows:

- a | width of input chute
- b | width of output chute
- c | depth of chamfer
- d | length of input chute
- e | horizontal location of left cavity wall
- f | position of center of tip of protuberance
- g | position of lower left corner of chute
- r | radius of protuberance
- $\theta$  | angle of input chute
- $\alpha$  | angle of chamfer

Given a rectangular peg of fixed dimensions, mass, and moment of inertia, the goal is to determine the design parameters such that a peg entering with different orientations (as shown in Figure 7 and Figure 8) always exits in the orientation with the center of gravity down. A secondary objective is to have the peg pass through the device as quickly as possible.

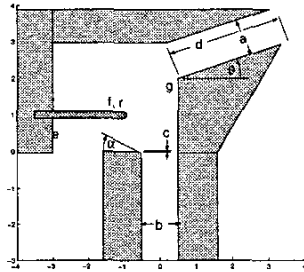


Fig. 6. Reorienting device with design variables taking on their initial values.

Let  $q_{\text{goal}}$  be a target configuration of the peg at some point well within the exit chute. Further, let  $T$  be the time when the peg either comes to rest or when the  $y$  component of its center of gravity moves below that of  $q_{\text{goal}}$ . The design problem can be expressed as an optimization problem with the design space specified by simple bounds placed on the 12 design variables and the objective function given as follows:

$$\mathcal{G} = \sum_{i=1}^2 w \|q_i(T_i) - q_{\text{goal}}\| + T_i \quad (15)$$

where  $w$  is a weight factor and  $i \in \{1, 2\}$  with 1 or 2 indicating that the peg entered the input chute with center of gravity on the left or right. With this objective function, the design problem can be written as

$$P = \min_P \mathcal{G}(X, T) \quad \text{s.t.} \quad \dot{X} = \mathcal{F}_Q(X, P), \quad (16)$$

where the parameter set  $P$  is the set of all the 12 design variables given at the beginning of this section, the states variable  $X \equiv (q, \dot{q})$ . In this design example, we use the ST model to compute  $\mathcal{F}_Q$  where  $Q$  represents the contact state set excluding the transitions from sustained contact to no contact. The objective function will be minimized when the peg fall through the device quickly and properly oriented.

The design was carried out in Matlab using the constrained optimization routine, `fmincon`, with the ST time-stepping method called twice for each objective function evaluation. The initial guess for the design is shown in Figures 7 and 8. Note that the peg comes to rest on the protuberance for both entering orientations. Figures 9 and 10 show the result obtained after approximately 1000 objective function evaluations. The weight factor  $w$  in the objective function is set to be 5. Note that the peg falls through the device in the proper orientation regardless of its entering orientation.

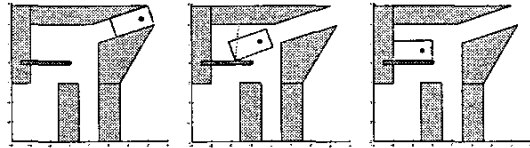


Fig. 7. Peg not able to pass through the device with initial design parameters with center of gravity starting on the right.

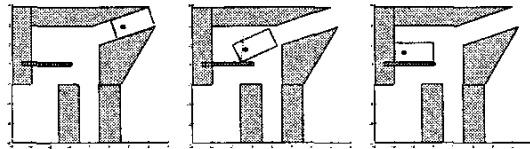


Fig. 8. Peg not able to pass through the device with initial design parameters with center of gravity starting on the left.

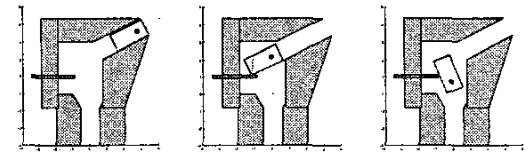


Fig. 9. Peg able to pass through the device with optimal design parameters with center of gravity starting on the right.

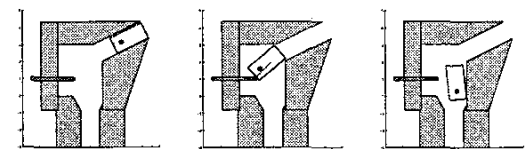


Fig. 10. Peg able to pass through the device with optimal design parameters with center of gravity starting on the left.

## VI. DISCUSSION

The problem of finding the feasible sets of design parameters and initial conditions for the assembly or part feeding processes is similar to the *motion planning problem* in robotics. Just as complete algorithms for motion planning are hard to obtain for complex problems, we may not be able to develop complete algorithms, or prove correctness or safety. We instead develop an algorithm that can be used for optimization of a system with nonsmooth dynamics in a nonconvex domain, obtaining locally-optimal, sufficing solutions.

We described two time-stepping models that can be applied not only for simulation and analysis, but also to solve design optimization problems. Both models can be used to solve the initial value problem that serves as the basis for the design optimization process as discussed in Section V. The ST model is more efficient computationally, because it leads to an LCP formulation, but it suffers from its inability to handle elastic impacts. To incorporate elastic impacts, one stops the ST model at the time of the impact, applies an impact model, resets the velocity variables, and resumes time stepping. In contrast, the SPK model incorporates elastic impacts but leads an NCP, which is difficult to solve.

If we replace the initial value problem in our design approach with a boundary value problem and impose the constraints of proper device function as part of the boundary conditions, we may be able to obtain a dynamically feasible design directly by solving a large boundary value problem. Unlike its initial-value counterpart, the boundary value problem is considerably more complicated. For one thing, it is no longer possible to decouple the time-stepping process into a finite sequence of individual subproblems each involving a single time step. Therefore, it is not possible to switch models or reset states (due to impact). Instead, one must consider the entire system along with the boundary conditions as a large-scale mixed complementarity problem. A unified formulation becomes necessary in order to deal with all types of contact transitions. The SPK model is, to the authors' knowledge, the only existing discrete model that allows us to plan motions with contact-state transitions. Preliminary results of the application of this method will be reported in a ICRA workshop [24].

### ACKNOWLEDGEMENT

The authors thank Michael Ferris for providing and supporting PATH and Todd Munson for his help on improving the AMPL/PATH input for the NCP model (14). This work is based on research supported by the National Science Foundation under Grants DMS-0139715 and DMS-0139701.

### REFERENCES

- [1] D. Stewart and J. Trinkle, "An implicit time-stepping scheme for rigid-body dynamics with inelastic collisions and coulomb friction," *International Journal of Numerical Methods in Engineering*, vol. 39, pp. 2673-2691, 1996.
- [2] P. Song, J.-S. Pang, and V. Kumar, "A semi-implicit time-stepping model for frictional compliant contact problems," *International Journal for Numerical Methods in Engineering*, to appear, 2003.
- [3] S. Akella, W. Huang, K. Lynch, and M. Mason, "Sensorless parts feeding with a one joint robot," in *Workshop on the Algorithmic Foundations of Robotics*, 1996.
- [4] J. Trinkle and J. J. Hunter, "A framework for planning dexterous manipulation," in *Proceedings of the 1991 IEEE International Conference on Robotics and Automation*, Apr. 1991, pp. 1245-1251.
- [5] J. Trinkle and D. Zeng, "Prediction of the quasistatic planar motion of a contacted rigid body," *IEEE Transactions on Robotics and Automation*, vol. 11, no. 2, pp. 229-246, Apr. 1995.
- [6] N. Zumel and M. Erdmann, "Nonprehensible two palm manipulation with non-equilibrium transitions between stable states," in *Proceedings of the 1996 IEEE International Conference on Robotics and Automation*, Apr. 1996, pp. 3317-3323.
- [7] B. R. Donald and D.-K. Pai, "On the motion of compliantly connected rigid bodies in contact: a system for analyzing designs for assembly," in *Proceedings of the 1990 IEEE International Conference on Robotics and Automation*, 1990, pp. 1756-1762.
- [8] D. Balkcom and J. Trinkle, "Computing wrench cones for planar rigid body contact tasks," *The International Journal of Robotics Research*, vol. 21, no. 12, pp. 1053-1066, 2002.
- [9] B. Mirtich, Y. Zhuang, K. Goldberg, J. Craig, R. Zanatta, B. Carlisle, and J. Canny, "Estimating pose statistics for robotic part feeders," in *Proceedings of the 1996 IEEE International Conference on Robotics and Automation*, 1996, pp. 1140-1146.
- [10] J. D. Wolter and J. Trinkle, "Automatic selection of fixture points for frictionless assemblies," in *Proceedings of the 1994 IEEE International Conference on Robotics and Automation*, vol. 1, May 1994, pp. 528-534.
- [11] T. Zhang and K. Goldberg, "Gripper point contacts for part alignment," *IEEE Transactions on Robotics and Automation*, vol. 18, no. 6, pp. 902-910, 2002.
- [12] M. Cherif and K. Gupta, "Planning quasi-static motions for reconfiguring objects with a multi-fingered robotic hand," in *Proceedings of the 1997 IEEE International Conference on Robotics and Automation*, April 1997.
- [13] B. Brogliato, *Nonsmooth Impact Mechanics - Models, Dynamics, and Control*. London: Springer-Verlag, 1996, lecture Notes in Control and Information Sciences.
- [14] P. Song, P. Kraus, V. Kumar, and P. Dupont, "Analysis of rigid-body dynamic models for simulation of systems with frictional contacts," *ASME Journal of Applied Mechanics*, vol. 68, pp. 118-128, 2001.
- [15] D. Stewart, "Rigid-body dynamics with friction and impact," *SIAM Review*, vol. 42, pp. 3-39, 2000.
- [16] J. Trinkle, J.-S. Pang, S. Sudarsky, and G. Lo, "On dynamic multi-rigid-body contact problems with coulomb friction," *Zeitschrift für Angewandte Mathematik und Mechanik*, vol. 77, no. 4, pp. 267-280, 1997.
- [17] K. Lynch, "Nonprehensile manipulation: Mechanics and planning," Ph.D. dissertation, School of Computer Science, Carnegie Mellon University, Mar. 1996.
- [18] G. Boothroyd and A. H. Redford, *Mechanized Assembly: Fundamentals of parts feeding, orientation, and mechanized assembly*. London: McGraw-Hill, 1968.
- [19] M. Anitescu and F. A. Potra, "A time-stepping method for stiff multibody dynamics with contact and friction," *International Journal of Numerical Methods in Engineering*, vol. 55, no. 7, pp. 753-784, 2002.
- [20] J. Trinkle, J. Tzitzouris, and J.-S. Pang, "Dynamic multi-rigid-systems with concurrent distributed contacts," *The Royal Society Philosophical Transactions: Mathematical, Physical and Engineering Sciences*, vol. 359, pp. 2575-2593, 2001.
- [21] M. S. Bazaraa and C. M. Shetty, *Nonlinear Programming: Theory and Algorithms*. New York: John Wiley & Sons, 1979.
- [22] P. R. Kraus, A. Fredriksson, and V. Kumar, "Modeling of frictional contacts for dynamic simulation," in *Proceedings of JROS 1997 Workshop on Dynamic Simulation: Methods and Applications*, 1997.
- [23] M. C. Ferris, R. Fourer, and D. M. Gay, "Expressing complementarity problems and communicating them to solvers," *SIAM Journal on Optimization*, vol. 9, pp. 991-1009, 1999.
- [24] P. Song, V. Kumar, and J.-S. Pang, "Contact models and numerical methods for simulation and optimization of processes with frictional contacts," Workshop on Multi-point Interaction in Robotics and Virtual Reality, IEEE International Conference of Robotics and Automation, 2004.